land

Article

Identification of Ground Deformation Patterns in Coal Mining Areas via Rapid Topographical Analysis

Zhen Du [1], Li Feng [1,*], Haiheng Wang [2], Ying Dong [3], Da Luo [4], Xu Zhang [1], Hao Liu [1] and Maosheng Zhang [1,*]

[1] School of Human Settlement Environment and Civil Engineering, Xi'an Jiaotong University, Xi'an 712000, China; duzhen@stu.xjtu.edu.cn (Z.D.); Zhangxuaa@stu.xjtu.edu.cn (X.Z.); liuhao309@stu.xjtu.edu.cn (H.L.)
[2] Software Engineering Center, The First Institute of Geographic Information Surveying and Mapping, Ministry of Natural Resources, Xi'an 710054, China; whhfgmimnr@163.com
[3] Key Laboratory of Loess Geological Hazards, Ministry of Natural Resources, Xi'an 710054, China; dongy@mail.cgs.gov.cn
[4] Shaanxi Key Laboratory of Ecological Restoration in North Shaanxi Mining Area, College of Life Sciences, Yulin University, Yulin 719000, China; luoda@yulinu.edu.cn
* Correspondence: fengli726@xjtu.edu.cn (L.F.); xjtzms@xjtu.edu.cn (M.Z.); Tel.: +861-87-0670-9218 (L.F.); +861-37-0921-2605 (M.Z.)

Abstract: Coal mining inevitably brings some negative impacts, such as surface subsidence, aquifer breakage, and land degradation, to the eco-geological environment in the mining area. Among these impacts, coal mining-induced ground deformation is the most serious and has threatened the geological, ecological, and human settlement securities of mining areas. Efforts existing in the literature apply to ground deformation identification in mined-out areas at the meso-/micro and short-time scales. However, when looking back at coal mining history, there are few ways to quickly and accurately quantify ground deformation at the regional and long-time scales. In this context, we propose a method for identifying ground deformation patterns in coal mining areas using historical high-precision digital elevation models (DEMs), including data preprocessing, DEM subtraction operations, interpretation, and fitting correction. This method was applied to the Yulin National Energy and Chemical Base and successfully identified the ground deformation characteristics of the Yulin coal mining area from 2015 to 2019. By determining surface subsidence displacement, excavation depth, stacking height, and the position of the goaf suspended roof area, the objective situation of ground deformation in Yulin mining area was obtained, and the mining methods and distribution characteristics of different surface deformations were analyzed and determined. The research results are of great significance for the development of mineral resources in mining areas, reducing geological disaster risks, protecting the ecological environment, and achieving the goal of coordinated development in mining areas.

Keywords: coal mining; ground deformation; elevation difference calculation; image interpretation; morphological patterns

check for updates

Citation: Du, Z.; Feng, L.; Wang, H.; Dong, Y.; Luo, D.; Zhang, X.; Liu, H.; Zhang, M. Identification of Ground Deformation Patterns in Coal Mining Areas via Rapid Topographical Analysis. *Land* **2023**, *12*, 1221. https://doi.org/10.3390/land12061221

Academic Editor: Giulio Iovine

Received: 18 May 2023
Revised: 8 June 2023
Accepted: 9 June 2023
Published: 12 June 2023

Copyright: © 2023 by the authors. Licensee MDPI, Basel, Switzerland. This article is an open access article distributed under the terms and conditions of the Creative Commons Attribution (CC BY) license (https://creativecommons.org/licenses/by/4.0/).

1. Introduction

As a leading industry in the world, the mining industry assumes the responsibility of providing energy and power for industrial enterprises and plays an important role in the development of national economies [1]. However, due to the gradual expansion of mining scale and the increasing sensitivity of public opinion to environmental protection issues, the number of geological problems in mining areas has gradually increased and become the focus of discussion [2]. The geological environment problems in mining areas are the deterioration phenomena caused or exacerbated by mining activities, including geological disasters, which are mainly caused by ground subsidence, landslides, and mudslides. Among these disasters, ground subsidence caused by coal mining is serious.

The ground subsidence in coal mining areas is from destroying the original stress balance of the surrounding rock mass after mining minerals, which leads to deformation, collapse, and crack development in the rock layer [3]. As a country that is rich in mineral resources, China has a coal industry that has experienced a 10-year golden development, with 100 large-scale coal mines, including over 70 coal mines with mining subsidence areas exceeding 4000 km^2. The total mining subsidence area formed has exceeded 20,000 km^2, and some resource-based cities have ground subsidence areas exceeding 10% of the total urban area [4]. Ground subsidence caused by coal mining is widely distributed in China and can cause serious damage to land, buildings, water resources, transportation, and other infrastructure within the mining area. To prevent and control the damage caused by coal mining subsidence, it is necessary to first identify and investigate the distribution and specific situation of the ground subsidence. With the gradual progress of related modern technologies, such as digital elevation models (DEMs) and satellite remote sensing, as well as the increasing demand for environmental governance in mining areas, the effective application of modern digital tools to solve geological environmental problems in mines has become an important means of current mining geological research [5].

There are many modern digital processing tools, among which the DEM is realized through digital image processing, digital photogrammetry, and various other technologies, and it is mainly used for large-scale movement detection and characterization, hazard assessment and susceptibility mapping, modeling, and monitoring [6]. Prior to its mature application in mining geological monitoring, the DEM underwent improvements and innovation from multiple perspectives. Mora et al. proposed a technique for generating deformable maps using synthetic aperture radar (SAR) data, which reduced the error of the DEM, and they tested the accuracy using European remote sensing SAR data [7]. Westoby et al. proposed a photogrammetric technique called the structure-from-motion (SfM) method and showed the vertical accuracy of this method by comparing a DEM derived using SfM with similar models obtained using ground laser scanning. Gradually, relevant technologies have been applied in mining geology [8]. Ge et al. applied a high-quality DEM to mining subsidence monitoring in seven active coal mining areas, demonstrating the feasibility of differential interferometric synthetic aperture radar (DINSAR) technology in mine subsidence monitoring [9]. Liu et al. used a high-resolution SAR database to monitor surface subsidence caused by repeated mining in mining areas using DINSAR and persistent scatterer interferometry (PSI), proving that the geocoding accuracy of a relief-DEM is superior. They concluded that PSI can further optimize the surface deformation boundary information obtained from the time series DINSAR [10]. Blachowski et al. proposed a DEM integration method for integrating a dense airborne laser scanning DEM with sparse photogrammetric data for larger areas by studying the error prediction of individual and fused terrain models, demonstrating a method for analyzing elevation changes in surface erosion areas after mining [11]. In addition, the geographic information system (GIS) provides a tool for various types of spatial analysis and graphical visualization of the results. Combined with a digital elevation model, GIS can better serve mine geological environment problems. Esaki et al. established a new three-dimensional settlement prediction method by combining random surface motion models and geographic information system (GIS) and then evaluated the settlement and geological damage caused by progressive horizontal strain [12]. Carabassa et al. used GIS technology to monitor gullies generated on slopes during the monitoring process of steep mountain breaks, helping to estimate DEM analysis before and after erosion and improving the monitoring process of mine restoration [13].

The rapid development of geographic information systems, digital image processing, digital photogrammetry, and other technologies has reduced the difficulty of identifying terrain and landforms in geological disaster research. These technologies have expanded the spatial range of ground information recognition, improved the accuracy and resolution of geological identification work, and provided clearer ideas for ecological regulation and restoration [14,15]. However, there are still various problems in the recognition of terrain and landforms using digital tools, such as differences between different sources

of digital elevation model data, making it difficult to handle them well. There is a high demand for identifying surface information, but it is difficult to obtain and organize surface information for regional and large-scale surface verification and restoration [16]. Obtaining large-scale and high-quality DEM data is also a major issue. In addition, radar interference technology is prone to incoherent phenomena (such as excavation depth and stacking height) in the identification process of large-gradient geological research. Therefore, it cannot obtain spatial deformation information with large surface gradients [17–19]. This will have a significant impact on the later identification and analysis process. Due to the inadaptability of various recognition technologies to the large-scale ground deformation verification work in mining areas, the current large-scale ground deformation verification work is mainly based on field verification, supplemented by relevant data from mining areas. Verification work requires a significant amount of manpower, material resources, financial resources, and time. The signs of ground deformation caused by coal mining become blurred with passaging time and human disturbances, which also brings great difficulties to field verification work. It is obviously not suitable to use conventional geodetic and traditional ground survey methods to obtain historical information about ground deformation in coal mining areas.

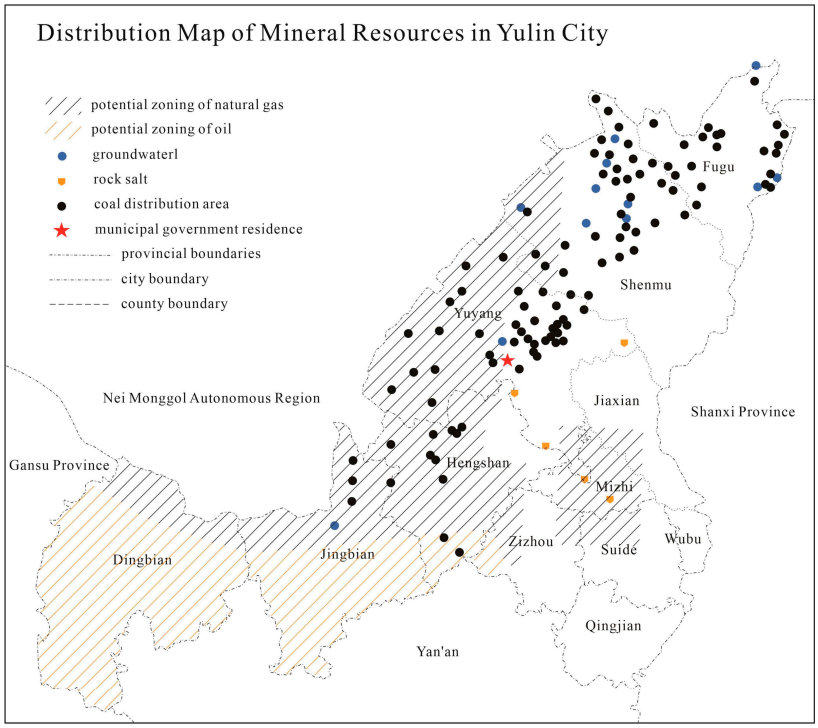
Based on the above current situation and problems, in this study, the Yulin Energy and Chemical Base in northern Shaanxi in the Ordos Basin was taken as an example. Based on the collection of high-precision DEM landscape data and mining area surface subsidence monitoring data, a new method was developed to quickly and accurately identify the scope and amount of coal mining subsidence using a multi-phase DEM and mining area monitoring data. This new method was applied to the Yulin National Energy Base, and the surface subsidence displacement, excavation depth, and stacking height of the coal mining area under different mining methods were determined for the first time, including the position and scope of the suspended roof area in the goaf. Overcoming the various incompatibilities between various recognition methods and large-scale mining area ground deformation recognition, compared with traditional ground deformation verification methods greatly reduces various costs such as time. The results provide data and technical support for identifying the degree and risk of the geological hazards caused by ground subsidence and for understanding the current situation of geological hazards in regional coal mining subsidence areas. It is of great significance to enhance the overall and timely nature of geological disaster prevention and control, protect people's lives and property, effectively promote ecological protection and restoration in mining areas, and optimize national spatial planning.

2. Materials and Methods

2.1. Overview of the Study Area

This study selected Yulin City, which is rich in mineral resources, as the research area. It is located at the northernmost point of Shaanxi Province, China, and faces the Yellow River to the east. It is in the Mesozoic and Cenozoic oil, gas, coal, and salt mineralization areas of the Ordos Basin and is a rare energy and mineral enrichment area in China and the world. Coal, oil, natural gas, rock salt, and other reserves are abundant, occupying an important position in the distribution of mineral resources nationwide, especially coal resources. The total amount of coal resources in the region is 271.4 billion tons, ranking among the top in the country, accounting for 83.12% of the total amount in Shaanxi Province and over 10% the total amount in China. The development potential of coal here is enormous, and the geological conditions are also very suitable for mining. The coal in the Yulin area was mainly formed during the Mesozoic and is in four formations: the Anding Formation, Zhiluo Formation, Yan'an Formation, and Fuxian Formation. These strata are a set of fluviolacustrine clastic rocks intercalated with coal deposits. The middle series comprises fluvial-lacustrine facies sandstones, pebbly sandstones, and interbedded layers of sandstone, shale, and mudstone with varying thicknesses, as well as coal seams and interbedded coal seams. The lower series comprises river marsh facies mudstone with

sandstone and a small amount of marl and sandstone, conglomerate, mudstone, and oil shale with thin coal seams (Figure 1). The overall terrain in Yulin is high in the northwest and low in the southeast, which varies in the range of 585–1905.1 m. The northwest wind beach area with abundant coal reserves has an altitude of 1200–1500 m, relatively, with flat terrain with small elevation differences, and a valley with a cutting depth of 5–30 m.



Stratum Horizon					Strata Thickness /m	Columnar Section
Erathem	System	Series	Formation	Code		
Cenozoic	Quaternary	Holocene Series		Qhal Qhal + 1	15 ~ 50	
			Maowusu	Qhm	0 ~ 20	
		Upper Pleistocene	Malan	Qp3eol	10 ~ 50	
			Salawusu	Qp3al + 1	0 ~ 160	
		Middle Pleistocene	Lishi	Qp2eol	30 ~ 160	
				Qp2al	10 ~ 30	
		Lower pleistocene	Wucheng	Qp1eol	10 ~ 50	
			Sanmen	Qp1al	10 ~ 20	
	Neogene	Pliocene Series	Baode	N2	0 ~ 80	
Mesozoic	Cretaceous	Lower Series	Rohan Cave	K1lh	0 ~ 120	
			Huanhe	K1h	0 ~ 600	
			Luohe	K1l	0 ~ 450	
	Jurassic System	Superior Series	Anding	J2a	360 ~ 650	
			Zhiluo	J2z		
		Middle-lower Series	Yan'an	J1-2y		
		Lower Series	Fuxian	J1f		
	Triassic System	Superior Series	Wayaobu	T3w	88 ~ 1756	
			Yongping	T3y		
			Hujiacun	T3h		
			Tongchuan	T3t		
		Middle Series	Zhifang	T2z		
		Lower Series	Heshanggou	T1h		
			Liujiagou	T1l		

Figure 1. Distribution of mineral resources and stratigraphic column for Yulin.

Yulin is at the junction of the Loess Plateau and the Mu Us Desert and is a typically ecologically fragile and sensitive area [20]. In recent years, the high-intensity mining of coal resources has led to large-scale land subsidence, which is widely distributed in the coal mining areas in Yulin. As of 2021, the area of the goaf settlement in Yulin had reached 1149 km^2 and was increasing at a rate of 100 km^2 per year [21]. The generation of land subsidence poses a serious threat to the ecological environment in the mining areas [22,23], and leads to water-related environmental effects such as damage to the groundwater system, a decrease in the groundwater level, interruption of surface water flow, and shrinkage of the wetland area in Yulin. In addition, the annual average precipitation in this area is far lower than the annual evaporation, and the total water resources are also very small. The water resources shortage has become the main constraint on the sustainable development of the regional energy industry. Water environment variations have led to a series of malignant impacts on the soil and vegetation development in Yulin, and the change of groundwater table could induce land subsidence [24–26]. Therefore, Yulin urgently needs to prevent and control the collapse risk of the goaf from the source. Its core lies in solving the problem of determining the location, type, development trend, and results of surface deformation areas in the Yulin goaf from the perspective of the mining history and how to support national spatial security. This is also an urgent need for the restoration of mining area geological environment governance, land reclamation, and optimization of national spatial planning.

2.2. Data and Preprocessing

The coal mines in Yulin are mainly distributed in four counties and districts: Yuyang, Shenmu, Hengshan, and Fugu. Therefore, in this study, we collected DEM data with a scale of 1:10,000 in 2019 (resolution: 2 m) for the four counties and districts; DEM data

with a 1:10,000 accuracy for four counties and districts in 2015 (resolution: 2 m); a 1:10,000 scale-combination table; a high-precision digital orthophoto image (DOM) of Yulin; the boundary of Yulin, distribution of the coal mining subsidence and suspended roof areas collected through coal mines, and the mining situation in the coal mining area. The collected DEM data were stored in a unified Chinese standard named frame format, so a series of preprocessing steps were necessary to meet the research needs, as shown in Figure 2.

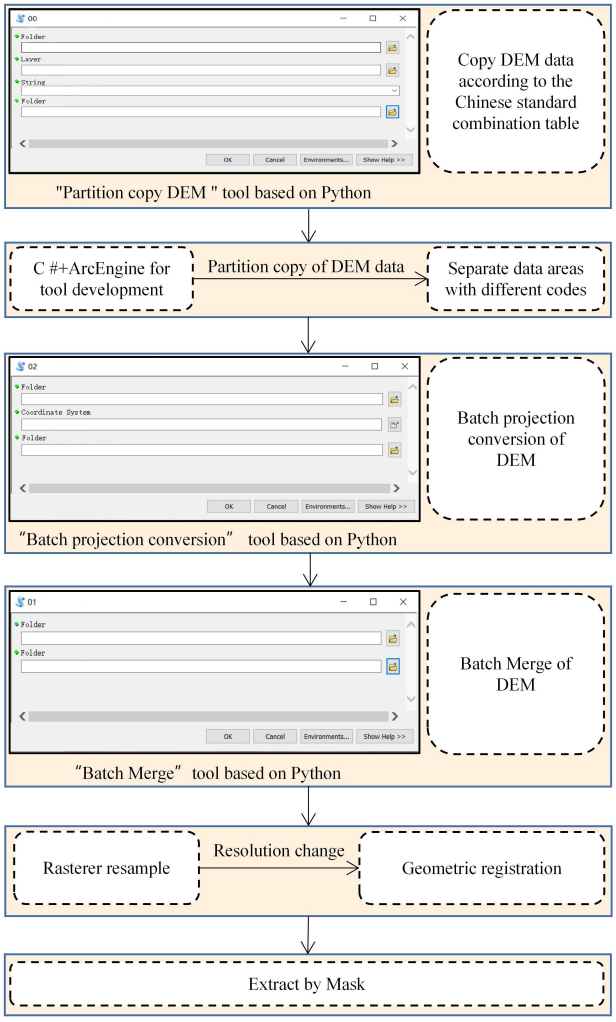


Figure 2. Flow chart of the preprocessing of the DEM data.

(1) DEM data were copied according to the Chinese standard combination table and the county boundary of the task area was matched to the combination table range to avoid errors and omissions in manually selecting DEM data in the task area. We used ArcGIS version 10.2 and a Python-based self-developed tool "Copy DEM Data Based on Combination Table" to complete the copying of the DEM data for the research area.

(2) The research area involves cross band data in the 1:10,000 Chinese standard data and cannot be directly fused. In order to accurately distinguish the cross band data based on the drawing number, a development method combining C# and ArcEngine and our and independently developed "Copy DEM Data in different bands" tool were applied. After running, the data with different codes was uniformly distinguished for further processing.

(3) Then, batch projection conversion of the DEM data was required. This study was based on Python and the independently developed "Batch Projection Conversion DEM" tool, which only requires setting the input and output paths. The projection coordinates with different data were uniformly converted to CGCS2000_ 3_ Degree_ GK_ Zone_ 37. The consistency of the spatial references of the DEM data was ensured.

(4) The converted DEM data were merged in batches. Using the self-developed "Batch Merge DEM" tool, the DEM was merged according to the county units to form the DEM datasets for the different districts and counties in different years.

(5) In order to adapt to the computing power of the workstation, improve the computational efficiency, and ensure consistent cell resolution when performing difference operations on the DEM data, raster resampling was performed on the two DEM datasets got. Through practical calculations and analysis, the DEM data resolution was re-sampled from 2 m to 5 m, and the difference operation was performed, resulting in an error of 0.01 m. This not only met the research requirements but also significantly improved the computational efficiency. Therefore, the DEM data with a resolution of 5 m was ultimately used.

(6) Because of errors in the production process and geometric deformation of the DEM results for the different years, there was a deviation in the position of the DEM. We used image registration, combined with manual and automatic selection of control points, to perform geometric registration of the DEM data for the two periods that required differences, ensuring that the positions of the two periods corresponded to each other.

(7) Finally, to ensure the one-to-one correspondence of the raster cells, the "Extract by Mask" tool in ArcGIS was used to conduct the mask extraction. The preprocessing of the DEM data before the difference calculation was completed.

2.3. DEM Subtraction Operation

After preprocessing the preliminary data, the Minus tool in the Spatial Analyst Tools provided in ArcToolbox was used to perform a difference operation on the two phases of DEM data. Taking the DEMs for Shenmu in 2019 and 2015 as examples, the DEM data for 2019 and 2015 were input into the parameter box, the output path was determined, and the calculations were started. The calculation results are shown in Figure 3. The format of the DEM data after the calculation was consistent with that of the preprocessed DEM data. The difference was that the raster cell values became settlement values and were no longer the elevation values in the original DEM. The ground deformation mentioned in this article refers to the vertical displacement of each point in the mining area.

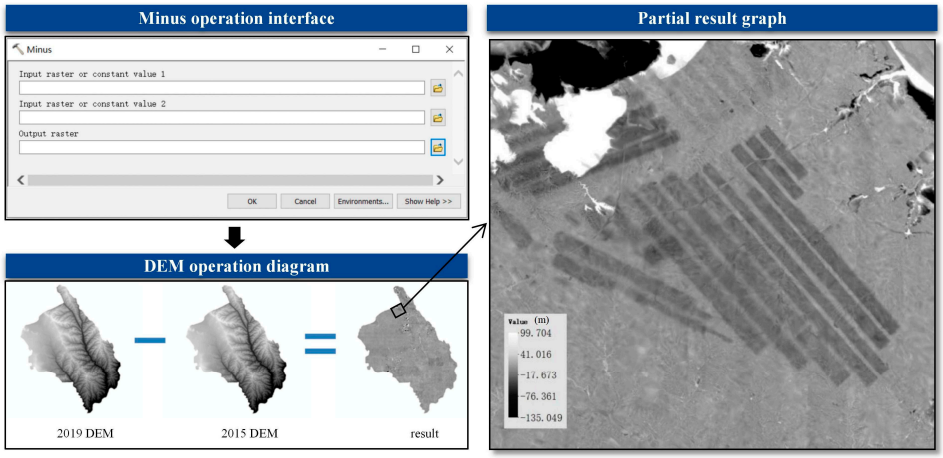


Figure 3. Diagram illustrating the DEM subtraction operation.

2.4. Interpretation

The DEM data obtained after the difference operation needed to be classified based on the ground deformation caused by different mining methods and to be reassigned with new values, namely, raster reclassification. The "Spatial Analyst Tools" → "Reclass" → "Reclassify" tools in ArcGIS were utilized to conduct the raster attribute table editing, reduce the pressure of the computer rendering raster data, and reduce the burden of the computer data processing. Based on the geological structure of the coalfield in the Yulin Energy and Chemical Industry Base in northern Shaanxi and the previous settlement

situation, ±10 m was taken as the critical value for reclassification. In addition, to avoid data redundancy, the parts with smaller DEM differences in the raster attribute table were removed.

Then, the reclassified raster data were converted into feature data using the "Raster to Polygon" tool in ArcGIS. To quickly process the raster data that generated the features, we used Python, and the independently developed "Statistics Raster Based on polygon" tool. This tool can achieve rapid extraction of the average settlement amount, maximum settlement amount, minimum settlement amount, and collapse volume within each polygon (Figure 4). Interpreting the DEM data after the difference was completed.

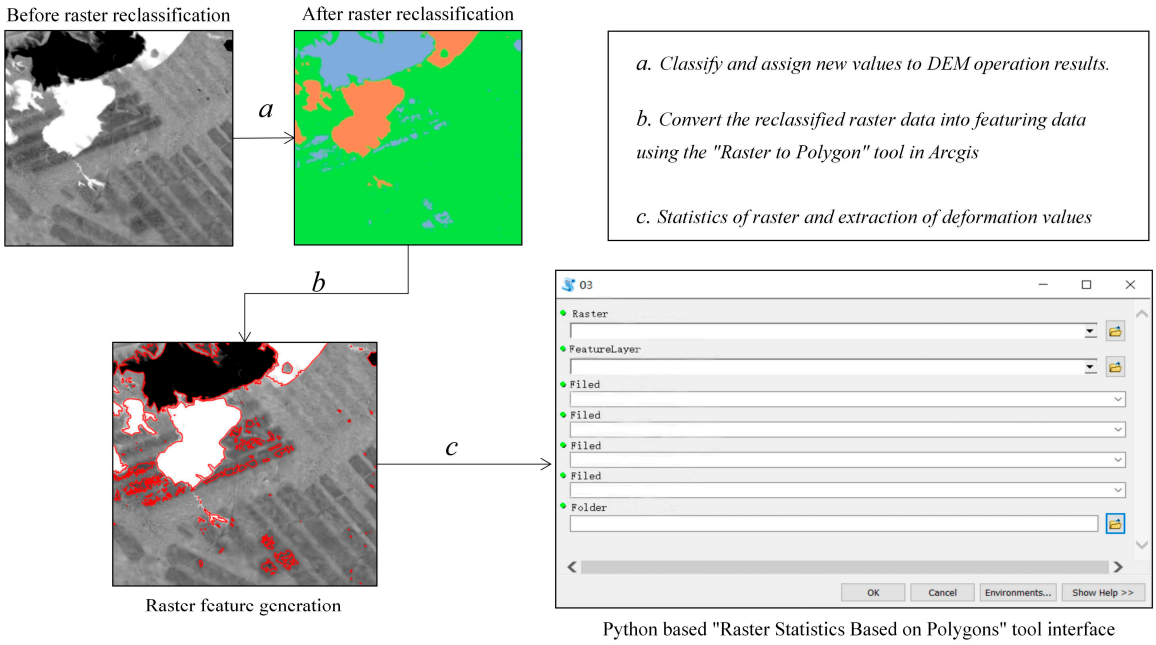


Figure 4. Diagram illustrating the DEM difference data interpretation process.

Differentiation of Different Ground Deformations and Mining Methods

1. Subsidence area caused by fully mechanized mining method

The different ground deformations exhibited different characteristics. The areas with collapsed areas as attribute values in the vector data results exhibited a very obvious gray and dark striped shape in the DEM data after the difference operation (Figure 5). These areas were manually judged and circled. Based on the process and principle of fully mechanized coal mining, it was found that the main method of fully mechanized mining in China is long arm mining. In this mining method, coal mining machines are used to break the coal in the excavation face, hydraulic supports are used to provide support, and scraper plates are used to convey the coal. The underground goaf formed is an interval strip. Based on the analysis of the collapse morphology in the DEM difference results, it was concluded that the areas with an obvious strip-like texture were the subsidence areas generated through application of the fully mechanized mining method.

2. Excavation and stack area generated by open-pit mining method

The areas with field attribute values of excavation and stack area in the vector data results were automatically interpreted and recognized by the computers. After the difference operation, the DEM results exhibited obvious features, i.e., white or black patches, and the average deformation value was >10 m. In the interpretation section of the difference DEM results, through raster reclassification, features generation, and writing statistical tools, the ground deformation range of the excavation and stack area was automatically identified. The black areas represented the excavation area, and the white areas represented the stack area. Large areas of abnormal deformation, such as borrow areas or building areas, may

be mistaken for open-pit coal mining areas, and comprehensive judgment needs to be made with the digital orthophoto map (DOM) (Figure 6a). Based on the mining history and mining engineering plan of the research area, it was found that all the large-scale severe deformations, except for the surface deformations caused by building houses, land reclamation, or other engineering projects, were excavation and stack areas generated by open-pit mining (Figure 6b).

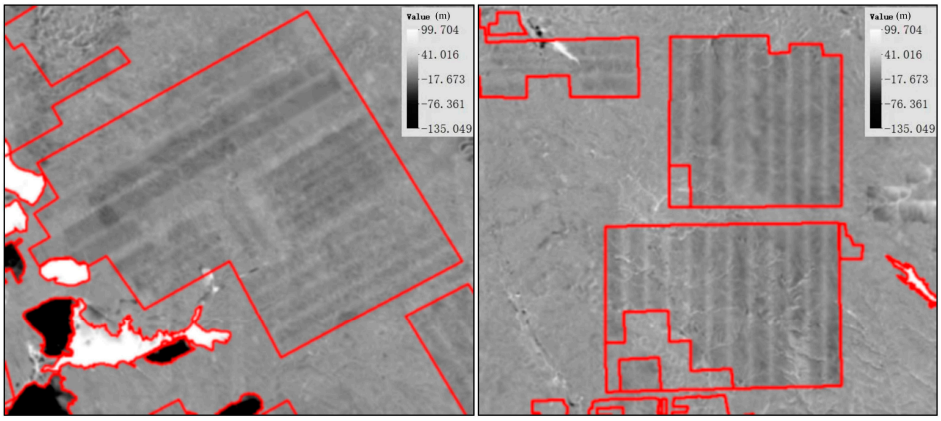
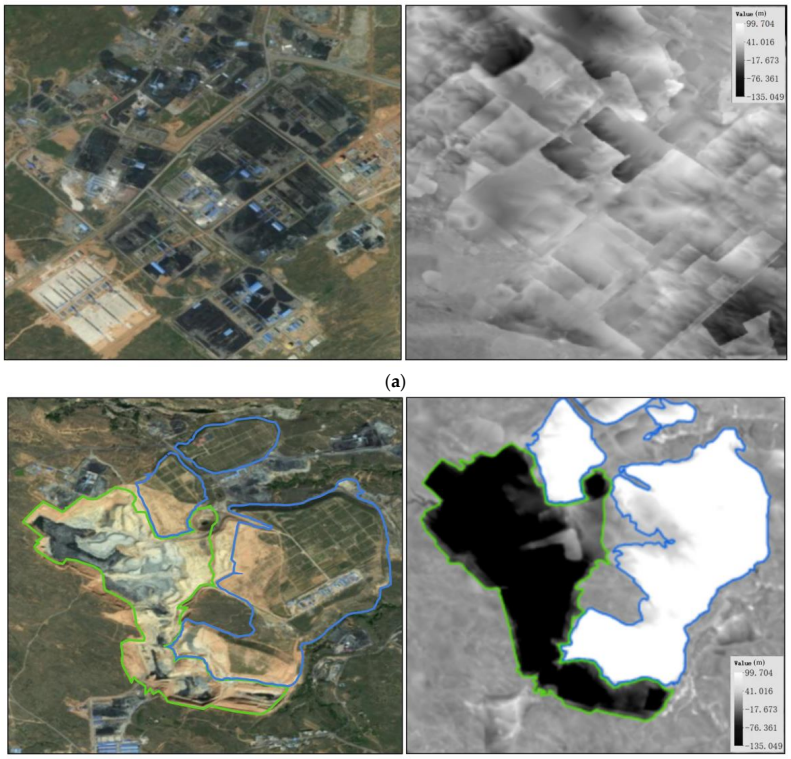


Figure 5. Diagram showing the identification result of the collapse range generated by the application of the fully mechanized mining method. The red boxes represent the collapsed area, and the color darkness of the strip represents the magnitude of deformation. The darker the color, the greater the deformation.



(**a**)

(**b**)

Figure 6. Comparison of ground deformation recognition between DOM and DEM. (**a**) Areas with significant deformation in DEM identification results due to the construction of ground buildings. The left image shows the digital orthophoto image of the building area, while the right image shows the DEM recognition results of the same area; (**b**) Areas with significant deformation in DEM identification results due to the excavation and stacking in the mining area.

3. Suspended roof area caused by room and pillar mining

The areas with field attribute values of a suspended roof area in the vector data results had indistinct features in the DEM difference results. We found the goaf based on the coal mining engineering plan, and we comprehensively analyzed the geological conditions of the coalfield in the study area to determine the underground subsidence situation in the area, thus determining the distribution of the suspended roof area in the Yulin mining area. According to the mining history of the Yulin mining area, the suspended roof area was generated by the room and pillar mining from 2015 to 2019. The suspended roof area is a major hidden danger and can lead to geological disasters in mining areas. Thus, the identification results can serve as a basis for on-site verification of the ground subsidence in the coal mining areas.

2.5. Fitting Correction

The accuracy of the ground deformation identification results obtained through DEM subtraction operation in Yulin City needs to be verified. Therefore, this article relies on the in situ monitoring station group set up in the coal mining area of the research area and uses the full time series ground deformation data obtained from monitoring to verify and correct the accuracy of the digital elevation model calculation results.

In order to obtain accurate and reliable observation data, it relies on ground deformation observation stations based on the global navigation satellite system (GNSS), which is equipped with real-time observation (monitoring) systems. This observation work mainly involves control network joint measurement, comprehensive observation, daily leveling, and determination of ground damage. During the control measurement phase, Ashtech static GPS was used to jointly measure the national C-level GPS points and multiple newly buried control points according to the E-level operation requirements. The plane coordinates of each point were obtained through calculation, and the elevation was the fitting elevation. At the same time, the electronic level was used to jointly measure the third level benchmark and the control points were arranged this time according to the third level requirements. After many independent observations, the average value was finally taken as the elevation of each control point. Finally, accurate and reliable full time series ground deformation observations within the study area were obtained through long-term observations, which serve as the standard for correcting DEM identification results.

Based on the terrain and model error distribution characteristics of the research area, the relationship between ground deformation observation values and DEM calculation results was analyzed. After a series of preprocessing of the DEM subtraction operation results, the two were fitted and calculated to obtain a fitting curve (Figure 7b). The results showed a positive correlation between the ground deformation values identified by DEM and the monitoring values. The coupling relationship between the ground deformation value calculated based on DEM and the monitoring value is proposed (Figure 7b), and the fitting accuracy is verified with the whole time series monitoring data validation. Based on the fitting relationship, more accurate ground deformation values for the entire mining area of Yulin were revised by calculating the DEM difference results (Figure 7c), and the authenticity and accuracy of the data results after correction were guaranteed. The high degree of matching between the range and depth displayed by the ground deformation recognition results and the measurement results shows the reliability and feasibility of this correction method. Thus, the newly developed method provides a good practical method for further batch recognition of ground deformation features in coal mining areas.

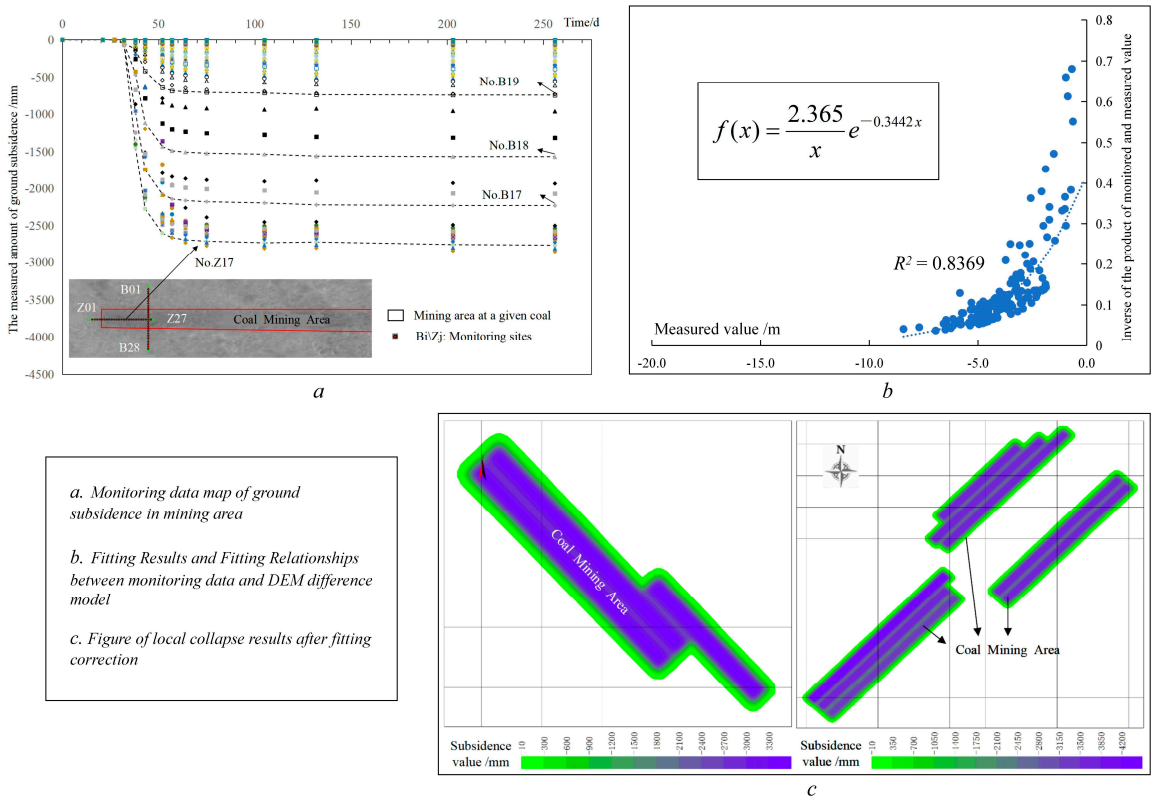


Figure 7. Flowchart of the DEM fitting calculation based on monitoring data.

3. Results

Based on the ground deformation values and dynamic characteristics of the mining area, as well as the different long-term coal mining methods and vector data for historical mines, computer automatic interpretation and manual interpretation were used to identify the ground deformation situation in the mining areas in the four counties and districts of Fugu, Shenmu, Yuyang, and Hengshan from 2015 to 2019, including: the range and amount of ground subsidence caused by the fully mechanized mining methods; the scope, deformation, and volume of the excavation and filling areas caused by open-pit mining; and the range of the suspended roof area caused by pillar mining. The range and amount of ground deformation caused by the different coal mining methods exhibited different ground deformation characteristics, and based on this, the objective situation of the ground deformation in the Yulin mining areas from 2015 to 2019 was grasped. After combining field monitoring data and the collected mining data on the distribution range of the subsidence areas in Yulin (Figure 8c), comparative analysis was conducted. It was found that the identified ground deformation results from the DEM difference data had high overlap with the previous distribution data for the subsidence areas, and the range was more accurate. Therefore, these results can be used as a basis for analyzing the distribution of the ground deformation in the coal mining areas in Yulin.

In this study, 256 coal mines were identified in four counties and districts, including the Yuyang, Hengshan, Shenmu, and Fugu Counties, with 3946 polygons. From 2015 to 2019, the total subsidence area increased by 343.26 km^2, the total suspended roof areas increased by 194.53 km^2, the total excavation area increased by 132.27 km^2, and the total landfill area increased by 112.04 km^2. In addition, because this calculation and identification was conducted using data from various counties and districts, the four counties and districts of Fugu, Shenmu, Yuyang, and Hengshan were arranged in sequence from north to south, reflecting the spatial differences in the ground subsidence in the Yulin mining areas from north to south. Therefore, the proportions of the ground deformation that were excavation area, stack area, collapse area, and suspended roof area in each of the four

counties and districts were calculated. In addition, the maximum amount of deformation that occurred in each county and district was calculated (Table 1). The distribution of the ground deformation in the mining areas from north to south in the study area is presented from both the horizontal and vertical angles in Figure 8.

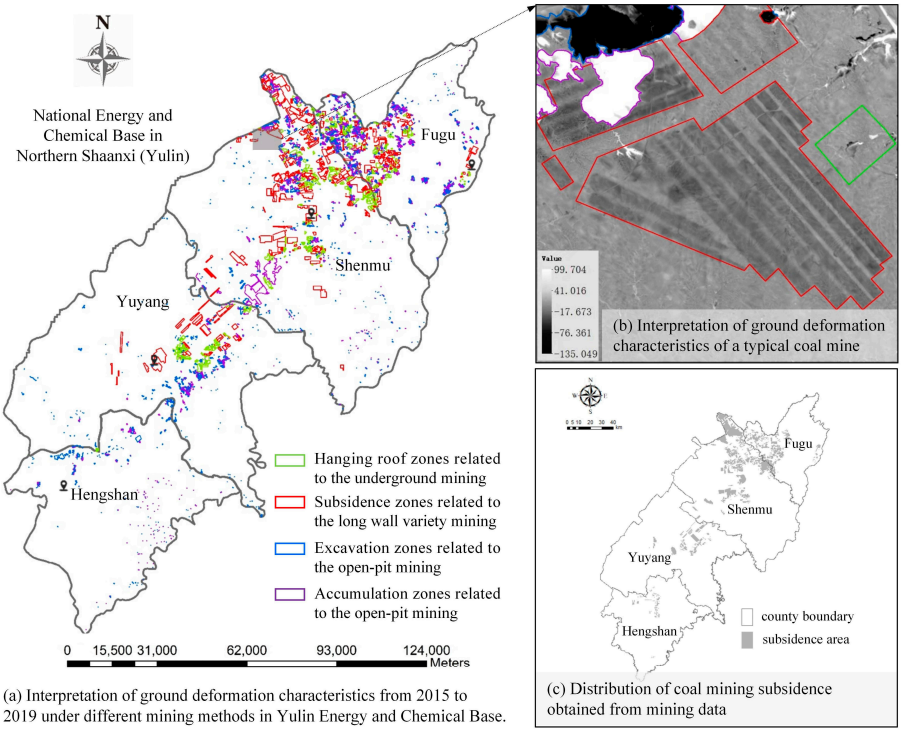


Figure 8. Recognition results and comparison of surface deformation features in the mining areas based on DEM.

Table 1. Statistics of ground deformation identification results for the Yulin coal mining area.

County/ District	Excavation Area (km^2)	Stack Area (km^2)	Subsidence Area (km^2)	Suspended Roof Area (km^2)	Maximum Excavation Depth (m)	Maximum Stacking Height (m)	Maximum Collapse Depth (m)
Fugu	43.57	43.51	30.82	40.50	107.12	94.35	36.80
Shenmu	46.81	51.94	271.70	104.89	171.02	132.02	39.97
Yuyang	22.21	11.69	40.74	49.14	107.04	110.83	25.57
Hengshan	19.68	4.89	0	0	53.72	54.23	0
Sum	132.27	112.04	343.26	194.53			

From the perspective of the horizontal distribution of the ground deformation in the mining areas, the ground deformation areas caused by coal mining in Yulin were mainly distributed in the northern part of Shenmu and the western part of Fugu, and a distribution zone composed of coal mining subsidence areas was formed along the southwest direction starting from in Shenfu mining area (Figure 8a). According to the statistics, the total identified excavation area in the Shenfu mining area was 90.38 km^2, the total stack area was 95.45 km^2, the total subsidence area was 302.52 km^2, and the total suspended roof area was 145.39 km^2, accounting for 68.33%, 85.20%, 88.13%, and 74.74% of the total surface deformation area in Yulin, respectively (Table 1). The main reason for this distribution is that the Shenfu mining area and the coal mining subsidence area trending in the southwest direction were characterized by thick coal seams, good coal quality, and shallow burial depths, which made it easy to mine the coal. The horizontal distribution of the ground

subsidence is related to the occurrence of the coal seams and the geological structure of the Yulin area.

From the perspective of the distribution of ground deformation in the Yulin mining area, the surface of the ground subsidence area caused by the fully mechanized mining appeared as obvious gray bands, while the profile curve exhibited regular undulation. After the mining of the working face, the mining areas were divided into a caving zone, fracture zone, and curved subsidence zone according to the different degrees of damage to the overlying rock [27,28]. The surface subsidence of the mining area exhibited the following trend: (1) The range of the subsidence gradually decreased downwards from the surface. (2) In a collapsed pit, the collapse value gradually increased from the edge to the center (as shown in the "Profile curve of subsidence area" in Figure 9). The excavation area and the stack area appeared as irregular black and white patches, respectively, and the profile curve exhibited significant and extensive fluctuations. However, the ground deformation characteristics of the suspended roof area were not obvious, and the profile map exhibited a gently undulating curve (Figure 9).

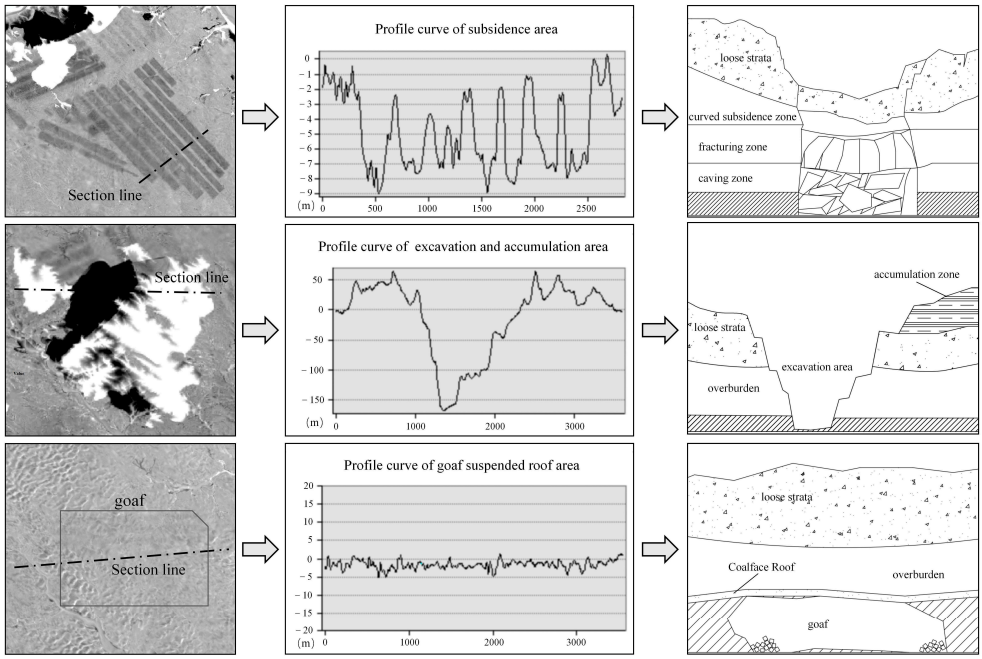


Figure 9. DEM map, deformation profile map, and collapse schematic diagram of different ground deformation areas in the mining area. From top to bottom, the sequence is the ground subsidence area caused by fully mechanized mining, the excavation and stacking area caused by open-pit mining, and the suspended roof area caused by pillar mining.

The results show that the subsidence density and value in the Shaanxi–Mongolia boundary zone, which is also in the Jurassic coalfield, are much lower than those in the central area of Yulin. The identification work yielded a maximum excavation depth of 171.02 m, a maximum stack height of 132.02 m, and a maximum collapse depth of 39.97 m throughout the entire area of Yulin, all of which occurred in the northern mining area of Shenmu. Moreover, the ground deformation was generally greater in the northern mining area than in the southern area of Yulin. The distribution of ground deformation in Yulin mining area shows this pattern because the coal seams here gradually become thinner from north to south and from west to east. This is caused by the influence of paleogeographic evolution on the coal accumulation and occurrence patterns of coal resources in the Jurassic coalfields in northern Shaanxi [29]. In addition, the overburden thickness of the Jurassic coalfields in northern Shaanxi gradually thinned from the hinterland to the edge, which was also an important factor affecting the spatial differences in collapse.

4. Discussion

4.1. Evaluation and Discussion of Ground Deformation Identification Methods

There are still technical bottlenecks in the detection of goaf and suspended roof areas. Due to the unclear deformation characteristics and the influence of vegetation coverage and human interference, the identification and exploration of goaf areas have always been a challenge for geological environment management in mining areas. In order to protect the geological environment of mining areas, many scientific and technological workers have performed extensive exploration and research work. Cao et al. combined 3D seismic exploration and transient electromagnetic methods to detect the area, shape, roof thickness, and height of the mined area, and used 3D laser scanning technology to visualize the hidden mined area [30]. Xue et al. reviewed the application and development of various methods of goaf detection, including seismic methods, high-density electrical methods, transient electromagnetic methods, ground penetrating radar, microseismic exploration, and radioactive methods [31]. However, goaf detection methods are mainly based on outdoor work, with a large workload in the field. Therefore, there is still a technical bottleneck in quickly and accurately identifying suspended roof area of goafs on a large scale.

The determination of the mining method for ground deformation in the mining area of Yulin City in this article is based on the geological conditions and mining history of Yulin. There are various explanations for the phenomenon of underground mining without significant surface subsidence. (1) A suspended roof area emerged after room and pillar mining. (2) After fully mechanized coal mining, the goaf formed a stable structure and did not collapse. (3) After mechanized coal mining, collapse occurred, but because the thickness of the overlying rock was much thicker than the mining thickness, the collapse did not extend to the surface [32,33]. Professor Zhang Maosheng's team analyzed the geological structure and mining history of the Yulin coalfield, summarized the corresponding relationship between different ground deformations and mining methods, and classified the ground deformations of the Yulin Energy and Chemical Base in northern Shaanxi. Their results show that only underground pillar mining will produce the phenomenon of goaf hanging but not collapsing in the short term after coal mining. After mechanized mining, collapse will occur. In addition, according to the analysis of ground subsidence mechanism in the Yushenfu mining area, when there is no discontinuous deformation of the ground and only slight subsidence occurs and forms a gentle basin, the ratio of the overlying rock thickness to the mining thickness needs to reach over 60. Therefore, based on the distribution of the coal seam thickness and overburden thickness in the Yulin coal mining area, the collapses caused by the fully mechanized mining in the North Shaanxi Energy and Chemical Industry Base will extend to the surface [34].

In addition, to prevent and control the hidden dangers and risks posed by the goaf caused by coal mining, the large coal mines in the Jurassic coalfield of northern Shaanxi should adopt the full caving method to manage the working face roof after adopting fully mechanized long arm mining, and the goaf should be filled with the forced or naturally caved surrounding rock. Overall, the goaf collapse caused by fully mechanized mining in the study area was rapid, and the surface deformation characteristics are obvious. Therefore, based on the DEM difference recognition results, we combined the mining range data of the coal mine area. If the recognition results within the mining range indicate no obvious ground deformation, it is determined that there is no significant collapse of the goaf; here, a suspended roof has formed in the goaf. Therefore, the method for identifying suspended roof areas proposed in this paper is reasonable and can meet the needs of the prevention and control of potential ground collapse risks in mining areas.

4.2. Limitations and Significance of the Method

However, the method used in this article to identify the surface deformation characteristics of the mining areas based on DEMs and mining area monitoring data has some shortcomings. In the process of DEM recognition of the surface deformation in the mining

area, the accuracy of the DEM data and the accuracy of the image registration are important factors affecting the accuracy of the surface deformation feature recognition. To improve the efficiency of the calculation and interpretation, we ultimately used DEM data with a resolution of 5 m, making it challenging to accurately ascertain small ground deformations. However, the research area included a wide range of regions and a large amount of data, making it difficult to ensure the accuracy of the different time registrations and multimodal registrations of the different data sources in the DEM differences. This is also the limitation of this method. In addition, the regional surface deformation feature recognition method proposed in this article is based on the entire DEM data of the study area and mining area monitoring data, and it needs to combine DOM data or optical remote sensing images for some areas to manually comprehensively determine the cause of the abnormal deformation in the study area. Using complete space–air–ground monitoring data as the data foundation also makes the implementation threshold of this method high and it has some limitations.

Despite the limitations mentioned above, to the best of our knowledge, this is the first time that multiple historical DEMs have been combined with monitoring data to identify the different surface deformation characteristics caused by different mining methods in the mining area throughout the city in the North Shaanxi Energy and Chemical Base. In addition, the proposed method is characterized by fast speed, efficiency, accuracy, and low cost. Therefore, it can provide a scientific basis for preventing and controlling geological disasters in mining areas.

4.3. Analysis of Spatial Characteristics of Ground Subsidence in Mining Areas

Over the years, scholars have investigated and studied geological disasters in Yulin and have found that the main cause of ground subsidence in the Yulin area is the high-intensity mining of coal [35,36]. This discovery verifies the consistent distribution of the coal mining and subsidence from the perspective of the horizontal distribution of the subsidence (Figure 10a). The results of this DEM recognition case study show that the ground deformation area caused by coal mining in Yulin has obvious spatial differences in terms of the horizontal distribution and subsidence degree. To verify and explain this spatial difference, several previous papers were referenced. Taking the Yushenfu area in Shaanxi Province as an example, Han et al. conducted a detailed analysis of the evolution of ground subsidence in mining areas. They concluded that the range of the subsidence basin above the goaf is much larger than that of the goaf, and the subsidence value is the largest in the center of the subsidence area and is the smallest at the edge of the subsidence area [36]. This verifies the results of the ground subsidence morphology identified in this study in the Yulin mining area. Fan et al. delineated 95 subsidence areas in the Yushenfu mining area in northern Shaanxi based on high-resolution satellite images and ground surveys, and they selected four factors, including the coal seam thickness, overlying rock thickness, mining intensity, and ground subsidence density, as evaluation indicators to evaluate ground subsidence in the Yushenfu mining area [35]. They formed a zoning map of the severity of the ground subsidence in the survey area (Figure 10c), which is highly consistent with the ground subsidence recognition results obtained in our study.

Through studying the geological structure of the coalfield in northern Shaanxi, it was found that the Jurassic coalfield in northern Shaanxi is in the northern part of the eastern wing of the Ordos Basin syncline, which is a monoclinic structure that dips gently towards the west, commonly known as the Shaanbei Slope. The ground is widely covered with modern eolian sand and Quaternary loess. These deposits are underlain by the Salawusu Formation, which has a wide distribution and large thickness and sporadic Neogene mudstone. Along the border of Shaanxi and Inner Mongolia, Cretaceous sandstone and mudstone are the underlying strata. Jurassic sandstone, mudstone, and coal measures are buried under Cretaceous, Neogene, and Quaternary strata or are exposed in river valleys. Overall, the coal seams in the hinterland of the Jurassic coalfield in northern Shaanxi, on the border between Shaanxi and Inner Mongolia, have a deep burial depth (Figure 10b). Currently, the coal mining area is at the edge of the Yushenfu mining area, which has a

smaller thickness of overlying strata and is easy to mine. Because of its unique coalfield occurrence conditions, such as a shallow burial depth, thick coal seams, and good coal quality, the Shenfu mining area serves as the central point for the distribution of the mining area. Therefore, the distribution of the ground deformation in the mining area in Yulin was formed consistently with the recognition results.

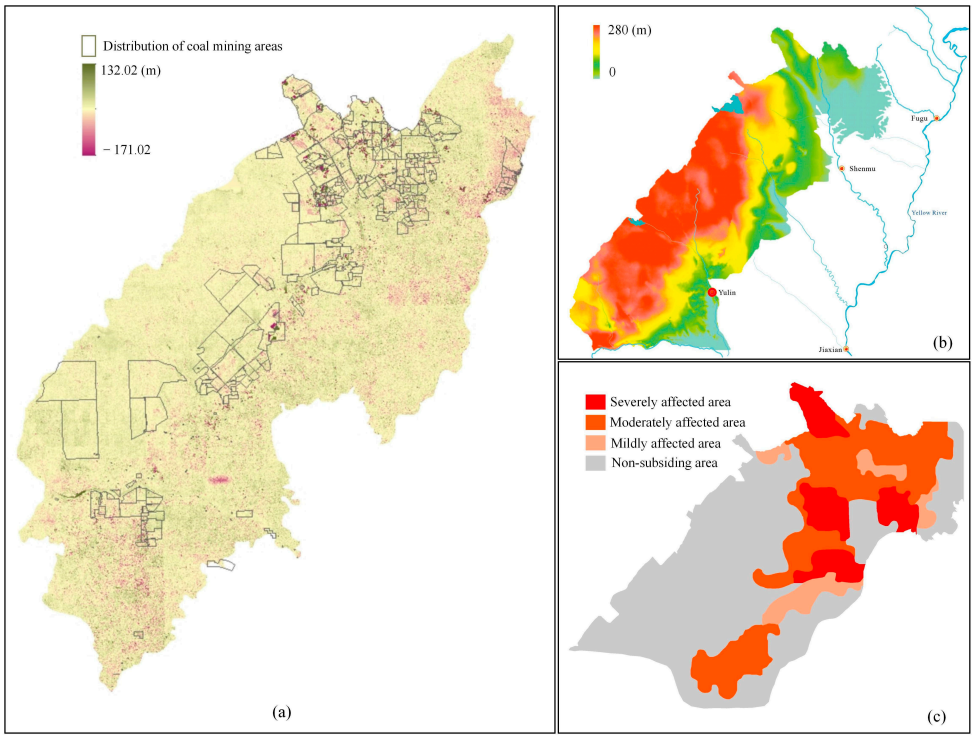


Figure 10. Zoning map of the coal mine distribution (**a**); overburden thickness distribution (**b**), and collapse severity (**c**) in the study area.

Yushenfu mining area in the Jurassic coalfield contains eight layers of coal, numbered from top to bottom as coal seams 1–8. The minable or partially minable coal seams are layers 3–7, which are in the Middle and Lower Jurassic Yan'an Formation. The Yan'an Formation is divided into five sections, each containing a coal group. Currently, the No. 1 and No. 2 coal formations in the upper part are shallowly buried and are the main mining targets. The fourth and fifth coal formations are deeply buried and have not been mined. The main minable coal seams in the Shenfu mining area in the northern part of Yulin are coal seams 1–2 and 2–2, which mainly comprise medium thick and thick coal seams. In addition, the Jurassic coalfields in northern Shaanxi are covered with sandy soil and loess cover, and the integrity of the rock mass overlying the coal seams is poor, with low physical and mechanical indicators. After coal mining, a large range of goaf will be generated. In the Shenfu mining area, where the thickness of the overlying rock layer is relatively small and the thickness of the coal seams is relatively large, the collapsed overlying rock blocks do not fill the large volume of the goaf, resulting in the continuous generation of new collapsed rock masses, which eventually extended to the surface. Therefore, the collapse value of the Shenfu mining area, especially the northern part of the Shenmu mining area, is relatively high.

5. Conclusions

This study developed a large-scale surface deformation feature recognition and analysis method based on DEM to achieve rapid and accurate recognition of surface deformation in coal mining areas. Taking Yulin City, which has abundant coal reserves, as an example, DEMs of various counties and districts in Yulin City in 2015 and 2019 were obtained. Using

computer automatic interpretation technology and manual intervention, a set of Python based automatic data analysis tools was independently developed, including DEM sorting, partition copying DEM, batch projection conversion DEM, and merging DEM. On this basis, preliminary digital elevation model data were preprocessed by using tools such as raster resampling, raster registration, and mask extraction in ArcGIS. Then, the Minus tool in the Spatial Analyst Tools provided by ArcToolbox was used to perform point-to-point elevation comparison subtraction on the processed DEM data. Raster reclassification, raster feature generation, and automatic extraction of the excavation and stack areas were performed on the DEM data after the difference operation. Based on this work, the DEM was used to manually locate the collapsed and suspended roof areas. By analyzing the correlation between the actual observation data in the mining area and the extracted DEM data, the fitting relationship was determined, and the average collapse amount, maximum collapse amount, minimum collapse amount, and collapse volume of each area were calculated and analyzed to obtain DEM based mining area ground deformation results. Finally, the range and deformation of land subsidence in the research area were obtained, and the horizontal distribution and morphological characteristics of land subsidence in the mining area were also obtained. The objective information about the ground deformation in the coal mining area in the North Shaanxi Energy and Chemical Industry Base from 2015 to 2019 was identified.

Regarding the application of the proposed method for identifying surface deformation features in mining areas, the rationality of the comprehensive judgment method for suspended roof areas mentioned in the recognition process was discussed. A more detailed explanation of the recognition method was provided for areas with unclear surface deformation features in the mining area. In addition, based on a large number of references, the accuracy of the recognition results was verified. A detailed analysis of the spatial distribution differences in various aspects such as the horizontal distribution and collapse degree obtained from the surface deformation recognition of the mining area in Yulin was conducted, and specific analysis and explanation were provided. This study provides a technical reference for the identification of large-scale ground deformation characteristics and contributes to the territorial space planning, the geological disasters prevention, and ecological restoration of the eco-geological environment in coal mining areas.

In the future, we will continue to study methods for identifying ground deformation in mining areas to improve the efficiency and accuracy of recognition. Due to limitations in the resolution of DEM raw data and the data processing capabilities of workstation computers, the recognition method proposed in this article still needs to be improved in terms of resolution, efficiency, and accuracy. Subsequent research can be improved in the following aspects: obtaining higher resolution DEM data; using workstation computing devices with stronger computing power; obtaining more field measurements of ground subsidence in mining areas to fit better curves and relationship expressions; and collecting more detailed coal mining data and the distribution of existing mining area subsidence to verify the accuracy of mining area surface subsidence. In addition, the recognition of ground deformation in mining areas will move towards a space–air–ground integrated network in the future, integrating satellite systems, aviation systems, and ground communication systems to comprehensively solve the key technological problems faced in the recognition of ground deformation in mining areas.

Author Contributions: Conceptualization, L.F. and M.Z.; methodology, L.F. and Y.D.; software, Z.D. and H.W.; formal analysis, Z.D., L.F., X.Z. and D.L; investigation, Z.D., X.Z. and H.L.; resources, H.W. and Y.D.; data curation, Z.D. and Y.D.; writing—original draft preparation, Z.D.; writing—review and editing, Z.D., L.F., D.L., H.L. and M.Z.; visualization, H.W.; supervision, H.W. and Y.D.; project administration, M.Z.; funding acquisition, M.Z. All authors have read and agreed to the published version of the manuscript.

Funding: This research was funded by the National Natural Science Foundation of China, grant number 42107209 and the National Key Research and Development Program of China, grant number 2018YFC1504700.

Institutional Review Board Statement: Not applicable.

Informed Consent Statement: Not applicable.

Data Availability Statement: The publicly available data is already shown in the figure, and other data cannot be disclosed due to the confidentiality of the data.

Conflicts of Interest: The authors declare no conflict of interest.

References

1. Muhire, I.; Manirakiza, V.; Nsanganwimana, F.; Nyiratuza, M.; Inzirayineza, T.A.; Uworwabayeho, A. The environmental impacts of mining on Gishwati Protected Reserve in Rwanda. *Environ. Monit. Assess.* **2021**, *193*, 600. [CrossRef]
2. Čechová, D.; Jarolímová, M.; Hummel, M.; Chvátal, O. Investigation into Flotation collector, montanol 551, concerning coal beneficiation plant of Paskov. *J. Min. Sci.* **2013**, *49*, 326–337. [CrossRef]
3. Hu, Q.; Cui, X.; Liu, W.; Feng, R.; Ma, T.; Li, C. Quantitative and dynamic predictive model for mining-induced movement and deformation of overlying strata. *Eng. Geol.* **2022**, *311*, 106876. [CrossRef]
4. Guo, W.; Hu, B.; Zhang, J.; Chen, Q.; Jia, X.; Li, J. Research on the Settlement Regulation and Stability of Large Building Foundation over Gobs: A Case Study in the Xiangcheng Coal Mine, China. *Shock. Vib.* **2021**, *2021*, 5533098. [CrossRef]
5. Li, J.; Chen, W. A rule-based method for mapping Canada's wetlands using optical, radar and DEM data. *Int. J. Remote Sens.* **2005**, *26*, 5051–5069. [CrossRef]
6. Jaboyedoff, M.; Oppikofer, T.; Abellán, A.; Derron, M.H.; Loye, A.; Metzger, R.; Pedrazzini, A. Use of LIDAR in landslide investigations: A review. *Nat. Hazards* **2012**, *61*, 5–28. [CrossRef]
7. Mora, O.; Mallorquí, J.; Broquetas, A. Linear and nonlinear terrain deformation maps from a reduced set of interferometric SAR images. *IEEE Trans. Geosci. Remote Sens.* **2003**, *41*, 2243–2253. [CrossRef]
8. Westoby, M.J.; Brasington, J.; Glasser, N.F.; Hambrey, M.J.; Reynolds, J.M. 'Structure-from-Motion' photogrammetry: A low-cost, effective tool for geoscience applications. *Geomorphology* **2012**, *179*, 300–314. [CrossRef]
9. Ge, L.; Chang, H.; Rizos, C. Mine subsidence monitoring using multi-source satellite SAR images. *Photogramm. Eng. Remote Sens.* **2007**, *73*, 1742–1745. [CrossRef]
10. Liu, Z.; Bian, Z.; Lei, S.; Liu, D.; Sowter, A. Evaluation of PS-DInSAR technology for subsidence monitoring caused by repeated mining in mountainous area. *Trans. Nonferrous Met. Soc. China* **2014**, *24*, 3309–3315. [CrossRef]
11. Blachowski, J.; Becker, M.; Kujawa, P.; Koźma, J.; Warchala, E.; Dynowski, A.; Pawlik, M.; Wajs, J.; Buczyńska, A. Transformation processes in lignite post-mining landscape—Erosion of anthropogenic formations in the former "Przyjazn Narodow—Szyb Babina" mine (Poland). *Z. Dtsch. Ges. Geowiss.* **2022**, *173*, 565–580. [CrossRef]
12. Esaki, T.; Djamaluddin, I.; Mitani, Y. A GIS-based prediction method to evaluate subsidence-induced damage from coal mining beneath a reservoir, Kyushu, Japan. *Q. J. Eng. Geol. Hydrogeol.* **2008**, *41*, 381–392. [CrossRef]
13. Carabassa, V.; Montero, P.; Alcañiz, J.M.; Padró, J.-C. Soil erosion monitoring in quarry restoration using drones. *Minerals* **2021**, *11*, 949. [CrossRef]
14. Uhlemann, S.; Smith, A.; Chambers, J.; Dixon, N.; Dijkstra, T.; Haslam, E.; Meldrum, P.; Merritt, A.; Gunn, D.; Mackay, J. Assessment of ground-based monitoring techniques applied to landslide investigations. *Geomorphology* **2016**, *253*, 438–451. [CrossRef]
15. Meng, X.; Qi, T.; Zhao, Y.; Dijkstra, T.; Shi, W.; Luo, Y.; Wu, Y.; Su, X.; Zhao, F.; Ma, J.; et al. Deformation of the Zhangjiazhuang high-speed railway tunnel: An analysis of causal mechanisms using geomorphological surveys and D-InSAR monitoring. *J. Mt. Sci.* **2021**, *18*, 1920–1936. [CrossRef]
16. Salmi, E.F.; Nazem, M.; Karakus, M. The effect of rock mass gradual deterioration on the mechanism of post mining subsidence over shallow abandoned coal mines. *Int. J. Rock Mech. Min. Sci.* **2016**, *91*, 59–71. [CrossRef]
17. Zhang, Y.; Meng, X.; Dijkstra, T.A.; Jordan, C.J.; Chen, G.; Zeng, R. Forecasting the magnitude of potential landslides based on InSAR techniques. *Remote Sens. Environ.* **2020**, *241*, 111738. [CrossRef]
18. Di Martire, D.; Novellino, A.; Ramondini, M.; Calcaterra, D. A-differential synthetic aperture radar interferometry analysis of a deep seated gravitational slope deformation occurring at bisaccia (Italy). *Sci. Total Environ.* **2016**, *550*, 556–573. [CrossRef]
19. Dong, L.; Wang, C.; Tang, Y.; Tang, F.; Zhang, H.; Wang, J.; Duan, W. Time series InSAR three-dimensional displacement inversion model of coal mining areas based on symmetrical features of mining subsidence. *Remote Sens.* **2021**, *13*, 2143. [CrossRef]
20. Guo, L.; Ren, Z.; Liu, Y. The causes of land landscape changes in semi-arid area of Northwest China: A case study of Yulin city. *J. Geogr. Sci.* **2006**, *16*, 192–198. [CrossRef]
21. Inspection Report on the Ecological Environment Management of Mines in Yulin City. Available online: http://www.ylzx.gov.cn/show.php?id=7815&cid=31 (accessed on 2 June 2023).
22. Luo, M.; Li, T. Spatial and temporal analysis of landscape ecological quality in Yulin. *Environ. Technol. Innov.* **2021**, *23*, 101700. [CrossRef]
23. Yang, Z.; Li, W.; Pei, Y.; Qiao, W.; Wu, Y. Classification of the type of eco-geological environment of a coal mine district: A case study of an ecologically fragile region in Western China. *J. Clean. Prod.* **2018**, *174*, 1513–1526. [CrossRef]

24. Hu, R.L.; Yue, Z.Q.; Wang, L.C.; Wang, S.J. Review on current status and challenging issues of land subsidence in China. *Eng. Geol.* **2004**, *76*, 65–77. [CrossRef]
25. Yu, H.; Gong, H.; Chen, B.; Liu, K.; Gao, M. Analysis of the influence of groundwater on land subsidence in Beijing based on the geographical weighted regression (GWR) model. *Sci. Total Environ.* **2020**, *738*, 139405. [CrossRef] [PubMed]
26. Ruiz-Constán, A.; Ruiz-Armenteros, A.M.; Martos-Rosillo, S.; Galindo-Zaldívar, J.; Lazecky, M.; García, M.; Sousa, J.J.; Sanz de Galdeano, C.; Delgado-Blasco, J.M.; Jiménez-Gavilán, P.; et al. SAR interferometry monitoring of subsidence in a detritic basin related to water depletion in the underlying confined carbonate aquifer (Torremolinos, southern Spain). *Sci. Total Environ.* **2018**, *636*, 670–687. [CrossRef]
27. Zhang, C.; Wang, F.; Bai, Q. Underground space utilization of coalmines in China: A review of underground water reservoir construction. *Tunn. Undergr. Space Technol.* **2021**, *107*, 103657. [CrossRef]
28. Liang, Y.; Ran, Q.; Zou, Q.; Zhang, B.; Hong, Y. Experimental study of mechanical behaviors and failure characteristics of coal under true triaxial cyclic loading and unloading and stress rotation. *Nat. Resour. Res.* **2022**, *31*, 971–991. [CrossRef]
29. Wang, S.; Fan, L.; Huang, Q.; Wang, G.; Shen, T. Coal water geological conditions and water conservation mining in Yushen mining area. *J. Xi'an Univ. Sci. Technol.* **2010**, *30*, 1–6. (In Chinese)
30. Cao, B.; Wang, J.; Du, H.; Tao, Y.; Liu, G. Research on comprehensive detection and visualize of hidden cavity goaf. *Sci. Rep.* **2022**, *12*, 22309. [CrossRef]
31. Xue, G.; Pan, D.; Yu, J. Review the applications of geophysical methods for mapping coal-mine voids. *Prog. Geophys.* **2018**, *33*, 2187–2192. [CrossRef]
32. Feng, D.; Hou, E.; Wang, S.; Xie, X.; Yuan, F.; Guo, L.; Wang, G.; Xie, Y.; Chen, Z. Research on 3D development characteristics of water-conducting fractured zone based on field measurement. *Front. Earth Sci.* **2022**, *10*, 808931. [CrossRef]
33. Wei, J.; Wang, S.; Song, S.; Sun, Q.; Yang, T. Experiment and numerical simulation of overburden and surface damage law in shallow coal seam mining under the gully. *Bull. Eng. Geol. Environ.* **2022**, *81*, 207. [CrossRef]
34. Zhang, M.; Dang, X. *Water Resources and Environmental Issues in Arid and Semiarid Regions*, 1st ed.; Science Press: Beijing, China, 2014; pp. 184–205.
35. Fan, L.; Ma, X.; Li, Y.; Li, C.; Yao, C.; Xiang, M.; Wu, B.; Peng, J. Geological disasters and control technology in high intensity mining area of western China. *J. Coal Ind.* **2017**, *42*, 276–285. [CrossRef]
36. Han, J.; Liu, H.; He, W. The evolution process of geological hazards in the ecologically fragile mining area of Yushenfu, Shaanxi. *Disaster Sci.* **2017**, *32*, 177–182. (In Chinese)

Disclaimer/Publisher's Note: The statements, opinions and data contained in all publications are solely those of the individual author(s) and contributor(s) and not of MDPI and/or the editor(s). MDPI and/or the editor(s) disclaim responsibility for any injury to people or property resulting from any ideas, methods, instructions or products referred to in the content.